Journal of Magnetic Resonance 201 (2009) 250–254

Contents lists available at ScienceDirect

Journal of Magnetic Resonance

journal homepage: www.elsevier.com/locate/jmr

Communication

Determination of the self-diffusion coefficient of intracellular water using PGSE NMR with variable gradient pulse length

Ingrid Åslund, Daniel Topgaard *

Physical Chemistry, Lund University, P.O. Box 124, SE-22100 Lund, Sweden

ARTICLE INFO

Article history:
Received 27 May 2009
Revised 27 August 2009
Available online 9 September 2009

Keywords:
PGSE
Self-diffusion
Short gradient pulse approximation
Cell water
Yeast

ABSTRACT

A new pulsed-gradient spin-echo NMR protocol for assessing the local self-diffusion coefficient D_0 of water confined within living cells is proposed. Equations for the apparent mean-square displacement $\langle Z^2 \rangle$ as a function of the effective diffusion time t_d and the duration of the displacement-encoding gradient pulses δ are derived. The standard method of estimating D_0 – reducing t_d until the influence of collisions between the water molecules and the plasma membrane can be neglected – often fails because of the small size of typical cells. As demonstrated here, the decrease of the apparent $\langle Z^2 \rangle$ with increasing δ at constant t_d can be utilized to measure D_0.

1. Introduction

The dynamic behavior of water within the living cell is a controversial subject. For example, recent neutron scattering studies on the halophilic organism *Haloarcula marismortui* indicate that the majority of the cell water has strongly reduced dynamics [1], while NMR relaxation dispersion experiments on the same type of cells show that most of the cell water reorient with a rate similar to bulk water [2].

One of the most powerful methods to study molecular motion is the pulsed-gradient spin-echo (PGSE) NMR technique [3–7]. For molecules confined in a pore, e.g. a cell, the experimental results depend on the local self-diffusion coefficient D_0 and the pore size and shape [8–11]. When trying to measure D_0 using PGSE NMR, the traditional approach has been to decrease the experimentally defined observational time scale, the diffusion time, in order to reduce the influence of collisions with the pore walls [12,13]. The analysis of PGSE NMR data is often based on the short gradient pulse (SGP) approximation which states that the molecular displacements taking place during the diffusion-encoding gradient pulses are insignificant in comparison to both the pore size and the displacements during the diffusion time [4,14,15]. A major problem when trying to study diffusion in cell-size structures is that the basic conditions for the SGP approximation no longer hold [16,17], thus giving rise to systematic errors in the estimated values of D_0 and the cell size [18].

Here we provide theoretical and experimental demonstrations of how the deviations from the SGP approximation can be utilized to determine D_0 for cell water, even in the presence of excess extracellular water. Proof-of-concept experiments are carried out on a loosely packed sediment of yeast cells. Within cell biology and biotechnology, yeast is one of the most intensely studied eukaryotic model organisms [19,20].

2. Theory

In the PGSE NMR experiment, the nuclear spin magnetization is dephased and rephased by two gradient pulses having the amplitude g and the duration δ. The time between the onset of the pulses is denoted Δ. In the SGP-limit, the echo attenuation $E(q,\Delta)$ is the Fourier transform of the average propagator $P(Z,\Delta)$ [4]:

$$E(q,\Delta) = \int_{-\infty}^{\infty} P(Z,\Delta)\exp(iqZ)dZ, \quad (1)$$

where q is $\gamma g\delta$, γ is the magnetogyric ratio of the observed nucleus, and Z is the displacement during the time Δ. The mean-square displacement $\langle Z^2 \rangle$ can be determined from the initial, low-q, decay of $E(q,\Delta)$:

$$E(q,\Delta) = \exp(-q^2\langle Z^2\rangle/2) \text{ (as } q \to 0) \quad (2)$$

Eq. (2) is independent of the functional form of $P(Z,\Delta)$, but only valid within the SGP approximation. If $P(Z,\Delta)$ is Gaussian, $\langle Z^2 \rangle$ can still be evaluated from Eq. (2) if Δ is replaced with an effective diffusion time $t_d = \Delta - \delta/3$.

* Corresponding author. Fax: +46 46 222 44 13.
E-mail address: daniel.topgaard@fkem1.lu.se (D. Topgaard).

1090-7807/$ - see front matter © 2009 Elsevier Inc. All rights reserved.
doi:10.1016/j.jmr.2009.09.006

The aim of this contribution is to show how deviations from Eq. (2), when using experimental parameters outside the range of validity of the SGP approximation, can be utilized to determine D_0 for cell water. With this goal in mind, let us define an apparent mean-square displacement $\langle Z(\delta,t_d)^2\rangle$ as

$$\langle Z(\delta,t_d)^2\rangle = -\frac{2}{\gamma^2\delta^2}\lim_{g\to 0}\frac{\partial \ln E}{\partial g^2} \tag{3}$$

in analogy with Eq. (2).

Neuman [21] presented a theory for calculating the echo attenuation resulting from a spin echo during a steady (e.g. not pulsed) gradient for a confined fluid with bulk diffusion coefficient D_0 under the assumption that the phase distribution of the nuclear spins remain Gaussian, the so-called Gaussian phase distribution (GPD) approximation. This assumption is equivalent to the condition $g \to 0$ as required by Eq. (3). Neuman's approach was applied to the PGSE experiment by Murday and Cotts [8], whose results were later extended to planar and cylindrical geometries by Balinov et al. [22] and van Gelderen et al. [23], respectively. The results for all of these geometries can be summarized as

$$\ln E = -2\gamma^2 g^2 \sum_{m=1}^{\infty} \frac{1}{\alpha_m^2(\alpha_m^2R^2+1-n_D)} \times \frac{2\alpha_m^2D_0\delta - 2 + 2L(\delta) + 2L(\Delta) - L(\Delta-\delta) - L(\Delta+\delta)}{(\alpha_m^2D_0)^2}. \tag{4}$$

In Eq. (4) $L(t) = e^{-\alpha_m^2 D_0 t}$, n_D is the number of dimensions (plane: $n_D = 1$, cylinder $n_D = 2$, sphere: $n_D = 3$), R denotes the half-spacing between the planes or the radius of the cylinder or the sphere, and α_m is the mth root of

$$J_{n_D/2}(\alpha_m R) - \alpha_m R J_{1+n_D/2}(\alpha_m R) = 0, \tag{5}$$

where J_ν is the νth order Bessel function of the first kind. Eq. (5) is equivalent to $\cos(\alpha_m R) = 0$ for the planar, $J_1'(\alpha_m R) = 0$ for the cylindrical, and $j_1'(\alpha_m R) = 0$ for the spherical case, where j_1 is the spherical Bessel function of the first kind.

The multiple propagator [24–26] and the step-wise gradient pulse [27] approaches can be used to calculate E for the full range of g, but for the purpose of this paper it is sufficient to focus on the low-g region in which Eq. (4) is valid. Inserting Eq. (4) into Eq. (3) yields

$$\langle Z(\delta,t_d)^2\rangle = 4\sum_{m=1}^{\infty} \frac{1}{\alpha_m^2(\alpha_m^2R^2+1-n_D)} \times \frac{2\alpha_m^2D_0\delta - 2 + 2L(\delta) + 2L(t_d+\delta/3) - L(t_d-2\delta/3) - L(t_d+4\delta/3)}{(\alpha_m^2D_0\delta)^2}. \tag{6}$$

By making series expansions of the $L(t)$ terms in Eq. (6), the following limiting behaviors are obtained:

$$\delta << \frac{R^2}{D_0} \Rightarrow \langle Z(\delta,t_d)^2\rangle = 4\sum_{m=1}^{\infty}\frac{1-L(t_d)}{\alpha_m^2(\alpha_m^2R^2+1-n_D)} \tag{7}$$

$$t_d << \frac{R^2}{D_0} \Rightarrow \langle Z(\delta,t_d)^2\rangle = 2D_0t_d \tag{8}$$

$$t_d >> \frac{R^2}{D_0} \Rightarrow \langle Z(\delta,t_d)^2\rangle = 8\sum_{m=1}^{\infty}\frac{1}{\alpha_m^2(\alpha_m^2R^2+1-n_D)} \times \frac{\alpha_m^2D_0\delta - 1 + L(\delta)}{(\alpha_m^2D_0\delta)^2} \tag{9}$$

$$\delta >> \frac{R^2}{D_0}, t_d >> \frac{R^2}{D_0} \Rightarrow \langle Z(\delta,t_d)^2\rangle = 8\sum_{m=1}^{\infty}\frac{1}{\alpha_m^4R^4(\alpha_m^2R^2+1-n_D)} \times \frac{R^4}{D_0\delta} = C\frac{R^4}{D_0\delta} \tag{10}$$

$$\delta << \frac{R^2}{D_0}, t_d >> \frac{R^2}{D_0} \Rightarrow \langle Z(\delta,t_d)^2\rangle = \frac{2}{2+n_D}R^2. \tag{11}$$

Of the expressions above, Eqs. 7, 8, and 11 are well-known from the literature [4]. The $n_D = 1$ version of Eq. (9) was introduced by Mitra and Halperin [28]. The long-δ and -t_d limit in Eq. (10) is the basis for the new approach of estimating D_0. The geometry dependent constant C in Eq. (10) equals 8/15 for the planar, 7/24 for the cylindrical, and 32/175 for the spherical case. Alternatively, Eq. (10) can be obtained from the results of Grebenkov [6]. The signal can be expressed as

$$E = \exp[-(\gamma g R T)^2\langle\phi^2/2\rangle], \tag{12}$$

where $\langle\phi^2/2\rangle$ is related to the mean square phase of the nuclear spins $\langle\varphi^2\rangle$ through

$$\langle\phi^2/2\rangle = \frac{\langle\varphi^2\rangle}{2(\gamma g R T)^2}, \tag{13}$$

and T is the time for echo formation. Comparing Eqs. (2) and (12) shows that

$$\langle Z^2\rangle = \frac{2R^2T^2}{\delta^2}\langle\phi^2/2\rangle. \tag{14}$$

In the limit $(D_0T/R^2) >> 1$, Grebenkov derived [6]

$$\langle\phi^2/2\rangle = 2\zeta_{-1}\frac{(\delta/T)}{(D_0T/R^2)} - 2\zeta_{-2}\frac{1}{(D_0T/R^2)^2}, \tag{15}$$

where ζ_{-1} and ζ_{-2} are constants depending on the pore geometry. For sufficiently large (D_0T/R^2), the second term can be neglected. Inserting the first term of Eq. (15) into Eq. (14) yields

$$\langle Z^2\rangle = 4\zeta_{-1}\frac{R^4}{D_0\delta}, \tag{16}$$

which is identical to Eq. (10) with $C = 4\zeta_{-1}$. Values of ζ_{-1} are tabulated in Ref. [6].

A plot of Eq. (6) and the regions of the (δ,t_d)-parameter space in which each approximation is valid are shown in Fig. 1. When $\delta << R^2/D_0$ and $t_d >> R^2/D_0$, $\langle Z(\delta,t_d)^2\rangle$ reaches a maximum value given by Eq. (11). Decreasing t_d or increasing δ both lead to a decreasing value of $\langle Z(\delta,t_d)^2\rangle$.

The most obvious way of determining D_0 is to perform the PGSE experiment in the short-t_d limit in accordance with Eq. (8). Due to instrumental limitations, such a direct approach is not feasible for cells being only a few micrometers in size. In the long-δ and long-t_d limit, Eq. (10), the value of $\langle Z(\delta,t_d)^2\rangle$ depends on the ratio R^4/D_0, having the paradoxical result that faster diffusion leads to an apparently smaller displacement! One very useful consequence of Eq. (10) is that, even if it is impossible to decrease δ and t_d to reach the short-t_d limit as required by Eq. (8), one can determine D_0 by varying δ at constant t_d. At short δ, the PGSE experiment is sensitive to R according to Eq. (11), while at longer δ the outcome of the measurement depends on the ratio R^4/D_0 consistent with Eq. (10).

Here, we propose the following protocol for determining D_0: Record E for a fixed value of t_d and a constant q-range for a series of values of δ centered at R^2/D_0. Since Eq. (4) is based on the assumption of perfectly reflecting barriers, the value of t_d should be much shorter than the characteristic time for molecular exchange across the cell membrane. The values of q should be chosen to give some decay of the intracellular signal while still being in the low-g/low-q range as required by Eq. (3). Fortunately, these conditions are easily fulfilled on modern NMR spectrometers with diffusion or microimaging capabilities. Similar protocols have previously been used to estimate the intracellular fraction in cell suspensions [29]

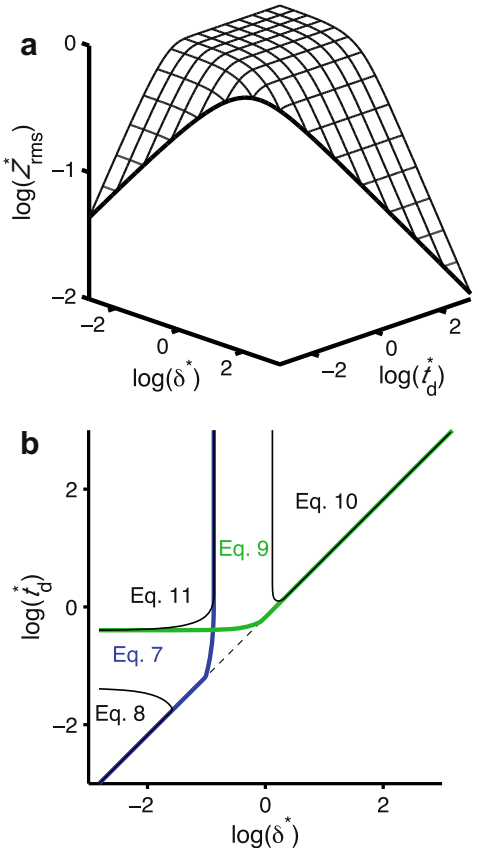

Fig. 1. (a) Reduced apparent root-mean-square displacement $Z_{rms}^* = \langle Z(\delta,t_d)^2\rangle^{1/2}/R$ as a function of the reduced gradient pulse length $\delta^* = \delta D_0/R^2$ and reduced effective diffusion time $t_d^* = t_d D_0/R^2$. The lines are calculated with Eq. (6) for a sphere ($n_D = 3$). The mesh with thin lines indicates constant δ^* or t_d^* while the thick line shows $\delta^* = 1.5t_d^*$ corresponding to a steady gradient in the PGSE experiment. (b) Areas of validity for the limiting behaviors in Eqs. (7)–(11). The regions of the (δ^*,t_d^*)-space in which each approximation deviates less than 10% from the true value is labeled with the corresponding equation number. The thin dashed line indicates $\delta^* = 1.5t_d^*$.

and the length scale of the director fluctuations in lyotropic lamellar phases [30].

3. Experimental

Fresh baker's yeast (Jästbolaget, Sweden) was dispersed in tap water in a weight ratio of 2:1 (yeast:water). The resulting viscous solution was transferred to a 5 mm O.D. disposable NMR tube and was stored in room temperature for 3 days. Just before NMR experiments the sample was centrifuged at 1500*g* for 2 min in order to remove CO_2 bubbles.

The NMR experiments were performed on a Bruker Avance-II 200 spectrometer operating at a ^{1}H resonance frequency of 200.13 MHz. The magnet was equipped with a Bruker DIF-25 probe capable of delivering *z*-gradients of approximately 9.6 T/m. The self-diffusion of water was monitored by observing the ^{1}H signal in a standard PGSE experiment [3]. The water signal was recorded for an array of values of δ and q while keeping t_d and the echo time TE fixed. With no signal averaging and 1 s repetition time, an entire data set to determine D_0 was acquired in about 3 min. Additional specific experimental details are given in the caption of Fig. 2. The experiments were performed at 5 temperatures linearly spaced between 5 and 25 °C using 25 min of equilibration after a temperature change. All data analysis was performed with Matlab.

4. Results and discussion

Experimental data obtained with the new protocol for a yeast cell suspension is shown in Fig. 2(a). The plot of NMR signal vs. q contains two clearly distinguishable components: (1) one component decaying at low q, corresponding to large displacements, being unaffected by the value of δ and (2) one component decaying at high q, corresponding to small displacements. Consistent with Eq. (10), this latter component is decaying at progressively higher q as δ is increased. Two components with similar behavior have previously been assigned to extra- and intracellular water, respectively [29]. Just as in Ref. [29], the accuracy of the gradients was checked by performing identical experiments on an aqueous polymer solution designed to give rise to two diffusion components with values similar to the ones observed in Fig. 2(a). For this reference sample, both components obey Gaussian diffusion statistics, Eq. (8), and the signal decays are independent of δ.

The measurements in Fig. 2(a) were analyzed by regressing

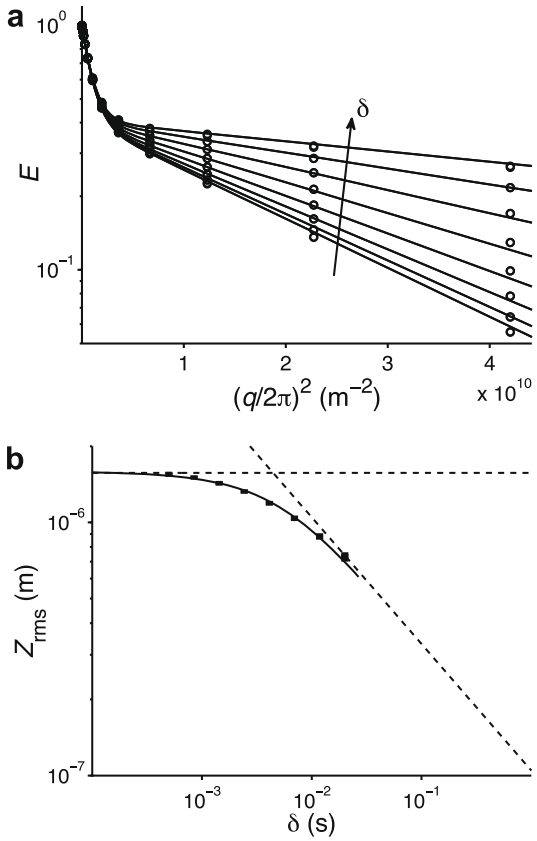

Fig. 2. Determination of the intracellular diffusion coefficient of water in yeast cells at 25.0 °C using PGSE NMR with variable gradient pulse length δ. (a) Water echo attenuation E vs. the wave vector q^2 for a set of δ (8 values in a logarithmic sequence between 0.5 and 20.0 ms). The arrow indicates the direction of increasing δ. The data was recorded for a constant effective diffusion time t_d = 20.0 ms and constant echo time TE = 50.0 ms. For the shortest δ, the gradient g was incremented in 15 logarithmically spaced steps from 1% to 100% of the maximum value 9.6 T/m. At longer δ, the gradient strength was reduced to keep the values of $q = \gamma g\delta$ constant. The circles are experimental data and the lines are the result of a model fit of Eq. (17) yielding intracellular diffusion coefficient $D_0 = 6.5 \pm 0.2 \times 10^{-10}$ m^{2}s^{-1}, extracellular diffusion coefficient $D_e = 1.268 \pm 0.007 \times 10^{-9}$ m^{2}s^{-1}, intracellular fraction $P_i = 0.407 \pm 0.002$, and cell radius $R = 2.48 \pm 0.01$ μm (confidence interval 67% using Monte Carlo error estimation). (b) Apparent root-mean-square displacement $Z_{rms} = \langle Z(\delta,t_d)^2\rangle^{1/2}$ vs. δ. The solid line is a plot of Eq. (6) using the values of D_0 and R obtained from the global fit. The vertical bars indicate the results from a fit where Z_{rms} was varied without the constraint of obeying Eq. (6). The vertical extension of the bars represent 80% confidence limits. The dashed lines are the short- and long-δ approximations calculated with Eqs. (11) and (10), respectively.

$$E(q,\delta) = (1 - P_i)\exp(-q^2 D_e t_d) + P_i \exp(-q^2 \langle Z(\delta, t_d)^2 \rangle / 2) \qquad (17)$$

onto the experimental data using the Levenberg–Marquardt algorithm [31]. In Eq. (17), P_i is the fraction of the intracellular component and D_e is the diffusion coefficient of the extracellular component. It should be noted that Eq. (17) is based on the assumption of negligible molecular exchange between the intra- and extracellular components on the time scale of t_d. The intracellular lifetime of water is about 0.5 s [32], which is an order of magnitude larger than the value of t_d used here.

The data was analyzed both with and without the constraint that $<Z(\delta,t_d)^2>$ is given by Eq. (6) where R and D_0 are unknown. As shown in Fig. 2(b), there is an excellent agreement between the two methods of analysis, indicating that Eq. (6) gives an accurate description of the variation of $<Z(\delta,t_d)^2>$ with δ. The plateau at short δ gives R according to Eq. (11) while the ratio R^4/D_0 is extracted from the decrease of $<Z(\delta,t_d)^2>$ at long δ in line with Eq. (10). In order to improve the accuracy of the fitted parameters, a global constrained fit was performed. In this fit $<Z(\delta,t_d)^2>$ was given by Eq. (6) which captures both the short- and long-δ behaviors in Eqs. (11) and (10), respectively. Thus, an equation with four adjustable parameters was fitted to the entire data set having two independent variables and in total 120 data points. As reported in the figure caption, the Monte Carlo method by Alper and Gelb [33] was used for error estimation. Due to the factor R^4/D_0 in Eq. (10), a small uncertainty of R results in a larger, although still acceptable, uncertainty of D_0.

A major problem when applying neutron scattering, NMR relaxation dispersion, and standard PGSE NMR to studies of cell water is the presence of extracellular water. In the current case, the diffusion of the extracellular component is only a factor of 2 faster than the intracellular one. Even if the NMR equipment would allow for experiments at the short t_d required for Eq. (8) to be valid, components with such small differences in decay rate would be impossible to resolve from the resulting bi-modal signal decay. The signal from the extracellular water can be suppressed by introducing a paramagnetic relaxation agent preferentially located in the extracellular space [12,34–36]. With the herein proposed protocol the values of t_d and δ are chosen to give at least an order of magnitude difference in decay rate of the two components, thus making them easy to resolve even without using relaxation agents.

At 25 °C the self-diffusion coefficient of bulk water is $D_b = 2.30 \times 10^{-9}\ m^2 s^{-1}$ [37,38]. The measured values $D_e = 1.27 \times 10^{-9}\ m^2 s^{-1}$ and $D_0 = 0.65 \times 10^{-9}\ m^2 s^{-1}$ correspond to the ratios $D_e/D_b = 0.55$ and $D_0/D_b = 0.29$. The reduced diffusion in the extracellular space can be attributed to the tortuosity of the pore space formed between the closely packed cells [39,40] and the presence of an extended polysaccharide cell wall outside the cell membrane [41]. The cell wall constitutes as much as 30% of the yeast cell dry weight [42], and can therefore be expected to have a significant influence on the extracellular water.

The measured value of D_0 agrees favorably with the extracellular relaxation-enhanced, short-t_d, PGSE experiments by Tanner [12]. We construe the reduction in comparison to bulk water as a result of the high concentration of macromolecules [43,44] and the presence of intracellular barriers such as the nuclear envelope, the endoplasmic reticulum, mitochondria, and vacuoles. It should be emphasized that D_0 as measured here corresponds to the diffusion in an infinite medium having the same composition and supramolecular organization as the intracellular space. The data is consistent with a single spherical membrane (i.e. the cell membrane) being the main barrier between the intra- and extracellular compartments. Although there are several intracellular subcompartments, water exchange between these seem to take place on a time scale shorter than the one given by the PGSE experiment (~1 ms). Since water reorientation [2,45] and molecular scale translational diffusion [46] is quite similar for cell- and bulk water, the values of D_0/D_b can be interpreted as an effective tortuosity of the crowded cell interior.

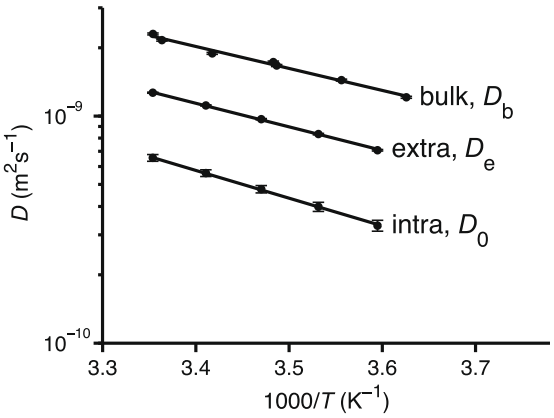

Fig. 3. Arrhenius plot of water self-diffusion coefficient D vs. inverse temperature $1/T$. The data points show measured values for intra- and extracellular water, D_0 and D_e, and literature data for bulk water D_b [38]. The error bars indicate 67% confidence interval. The solid lines show the results of fitting the Arrhenius equation, yielding the activation energies $E_a = 18.5 \pm 0.4$ kJ/mol for D_b, $E_a = 19.9 \pm 0.3$ kJ/mol for D_e, and $E_a = 23 \pm 2$ kJ/mol for D_0 (67% confidence).

The temperature dependence of D_b, D_e, and D_0 in the interval +5 to +25 °C and the corresponding Arrhenius analysis is shown in Fig. 3. Although both D_e and D_0 are reduced in comparison to D_b, identical activation energies E_a would be expected if the reduction was purely the result of geometrical obstruction effects. The obtained values of E_a are indeed almost the same, indicating similar diffusion mechanisms on the molecular scale. The slightly higher value of E_a for intracellular diffusion could be interpreted in terms of stronger interactions between the water and intracellular solutes. Such an interpretation should be taken with caution due to the problems associated with an Arrhenius analysis applied to a living system that quite possibly responds to a change in temperature.

5. Conclusions

A PGSE NMR protocol with varying gradient pulse length δ can be used to estimate the local self-diffusion coefficient of molecules confined in micrometer-size objects in general, and biological cells in particular, using only a few minutes of instrument time. For cell water, the results could be used as a probe of the intracellular organization. The protocol is easy to implement on any modern NMR spectrometer, or even bench-top NMR system, with diffusion accessories.

Acknowledgments

This work is financially supported by the Swedish Foundation for Strategic Research (SSF) and the Swedish Research Council (VR) through the Linnaeus Center of Excellence on Organizing Molecular Matter (OMM). We are grateful to an anonymous reviewer for providing the exact values of the coefficient C in Eq. (10) and pointing out the connections between the work presented here and that in Ref. [6].

References

[1] M. Tehei, B. Franzetti, K. Wood, F. Gabel, E. Fabiani, M. Jasnin, M. Zamponi, D. Oesterhelt, G. Zaccai, M. Ginzburg, B.-Z. Ginzburg, Neutron scattering reveals extremely slow cell water in a Dead Sea organism, Proc. Natl. Acad. Sci. USA 104 (2007) 766–771.

[2] E. Persson, B. Halle, Cell water dynamics on multiple time scales, Proc. Natl. Acad. Sci. USA 105 (2008) 6266–6271.
[3] E.O. Stejskal, J.E. Tanner, Spin diffusion measurements: spin echoes in the presence of a time-dependent field gradient, J. Chem. Phys. 42 (1965) 288–292.
[4] P.T. Callaghan, Principles of Nuclear Magnetic Resonance Microscopy, Clarendon Press, Oxford, 1991.
[5] W.S. Price, Pulsed-field gradient nuclear magnetic resonance as a tool for studying translational diffusion: Part 1. Basic theory, Concepts Magn. Reson. 9 (1997) 299–336.
[6] D.S. Grebenkov, NMR survey of reflected Brownian motion, Rev. Mod. Phys. 79 (2007) 1077–1137.
[7] D. Topgaard, Probing biological tissue microstructure with magnetic resonance diffusion techniques, Curr. Opin. Colloid Interface Sci. 11 (2006) 7–12.
[8] J.S. Murday, R.M. Cotts, Self-diffusion coefficient of liquid lithium, J. Chem. Phys. 48 (1968) 4938–4945.
[9] J.E. Tanner, E.O. Stejskal, Restricted self-diffusion of protons in colloidal systems by the pulsed-gradient, spin-echo method, J. Chem. Phys. 49 (1968) 1768–1777.
[10] D.G. Cory, A.N. Garroway, Measurement of translational displacement probabilities by NMR – an indicator of compartmentation, Magn. Reson. Med. 14 (1990) 435–444.
[11] D. Topgaard, O. Söderman, Experimental determination of pore size and shape using *q*-space NMR microscopy in the long diffusion-time limit, Magn. Reson. Imaging 21 (2003) 69–76.
[12] J.E. Tanner, Intracellular diffusion of water, Arch. Biochem. Biophys. 224 (1983) 416–428.
[13] W. Heink, J. Kärger, G. Fleischer, J. Rauchfuß, PFG NMR self-diffusion measurements with large field gradients, J. Magn. Reson. A 114 (1995) 101–104.
[14] J. Kärger, W. Heink, The propagator representation of molecular transport in microporous crystallites, J. Magn. Reson. 51 (1983) 1–7.
[15] P.P. Mitra, P.N. Sen, L.M. Schwartz, P. Le Doussal, Diffusion propagator as a probe of porous media, Phys. Rev. Lett. 68 (1992) 3555–3558.
[16] P. Linse, O. Söderman, The validity of the short-gradient-pulse approximation in NMR studies of restricted diffusion, simulations of molecules diffusing between planes, in cylinders and spheres, J. Magn. Reson. A 116 (1995) 77–86.
[17] C. Malmborg, D. Topgaard, O. Söderman, NMR diffusometry and the short gradient pulse approximation, J. Magn. Reson. 169 (2004) 85–91.
[18] W.S. Price, P. Stilbs, O. Söderman, Determination of pore space shape and size in porous systems using NMR diffusometry. Beyond the short gradient pulse approximation, J. Magn. Reson. 160 (2003) 139–143.
[19] W.H. Mager, J. Winderickx, Yeast as a model for medical and medicinal research, Trends Pharmacol. Sci. 26 (2005) 265–273.
[20] M. Menacho-Marquez, J.R. Murguia, Yeast on drugs: *Saccharomyces cerevisiae* as a tool for anticancer drug research, Clin. Transl. Oncol. 9 (2007) 221–228.
[21] C.H. Neuman, Spin echo of spins diffusing in a bounded medium, J. Chem. Phys. 60 (1974) 4508–4511.
[22] B. Balinov, B. Jönsson, P. Linse, O. Söderman, The NMR self-diffusion method applied to restricted diffusion. Simulation of echo attenuation from molecules in spheres and between planes, J. Magn. Reson. A 104 (1993) 17–25.
[23] P. van Gelderen, D. DesPres, P.C.M. van Zijl, C.T.W. Moonen, Evaluation of restricted diffusion in cylinders. Phosphocreatine in rabbit leg muscle, J. Magn. Reson. B 103 (1994) 255–260.
[24] A. Caprihan, L.Z. Wang, E. Fukushima, A multiple-narrow-pulse approximation for restricted diffusion in a time-varying field gradient, J. Magn. Reson. A 118 (1996) 94–102.
[25] P.T. Callaghan, A simple matrix formalism for spin echo analysis of restricted diffusion under generalized gradient waveforms, J. Magn. Reson. 129 (1997) 74–84.
[26] S.L. Codd, P.T. Callaghan, Spin echo analysis of restricted diffusion under generalized gradient waveforms: planar, cylindrical, spherical pores with wall relaxivity, J. Magn. Reson. 137 (1999) 358–372.
[27] A.V. Barzykin, Theory of spin echo in restricted geometries under a step-wise gradient pulse sequence, J. Magn. Reson. 139 (1999) 342–353.
[28] P.P. Mitra, B.I. Halperin, Effects of finite gradient-pulse widths in pulsed-field-gradient diffusion measurements, J. Magn. Reson. A 113 (1995) 94–101.
[29] C. Malmborg, M. Sjöbeck, S. Brockstedt, E. Englund, O. Söderman, D. Topgaard, Mapping the intracellular fraction of water by varying the gradient pulse length in *q*-space diffusion MRI, J. Magn. Reson. 180 (2006) 280–285.
[30] I. Åslund, C. Cabaleiro-Lago, O. Söderman, D. Topgaard, Diffusion NMR for determining the homogeneous length scale in lamellar phases, J. Phys. Chem. B 112 (2008) 2782–2794.
[31] W.H. Press, S.A. Teukolsky, W.T. Vetterling, B.P. Flannery, Numerical Recipes: The Art of Scientific Computing, Cambridge University Press, New York, 2007.
[32] I. Åslund, A. Nowacka, M. Nilsson, D. Topgaard, Filter-exchange PGSE NMR determination of cell membrane permeability, J. Magn. Reson. 200 (2009) 291–295.
[33] J.S. Alper, R.I. Gelb, Standard errors and confidence intervals in nonlinear regression: comparison of Monte Carlo and parametric statistics, J. Phys. Chem. 94 (1990) 4747–4751.
[34] J. Andrasko, Measurement of membrane permeability to slowly penetrating molecules by a pulse gradient NMR method, J. Magn. Reson. 21 (1976) 479–484.
[35] C. Labadie, J.-H. Lee, G. Vetek, C.S. Springer Jr., Relaxographic imaging, J. Magn. Reson. B 105 (1994) 99–112.
[36] M.D. Silva, K.G. Helmer, J.-H. Lee, S.S. Han, C.S. Springer Jr., C.H. Sotak, Deconvolution of compartmental water diffusion coefficients in yeast-cell suspensions using combined T1 and diffusion measurements, J. Magn. Reson. 156 (2002) 52–63.
[37] M. Holz, S.R. Heil, A. Sacco, Temperature-dependent self-diffusion coefficients of water and six selected molecular liquids for calibration in accurate ^{1}H NMR PFG measurements, Phys. Chem. Chem. Phys. 2 (2000) 4740–4742.
[38] W.S. Price, H. Ide, Y. Arata, Self-diffusion of supercooled water to 238 K using PGSE NMR diffusion measurements, J. Phys. Chem. A 103 (1999) 448–450.
[39] J. Hrabe, S. Hrabetova, K. Segeth, A model of the effective diffusion and tortuosity in the extracellular space of the brain, Biophys. J. 87 (2004) 1606–1617.
[40] B. Jönsson, H. Wennerström, P.G. Nilsson, P. Linse, Self-diffusion of small molecules in colloidal systems, Colloid Polym. Sci. 264 (1986) 77–88.
[41] M. Osumi, The ultrastructure of yeast: cell wall structure and formation, Micron 29 (1998) 207–233.
[42] P.N. Lipke, R. Ovalle, Cell wall architecture in yeast: new structure and new challenges, J. Bacteriol. 180 (1998) 3735–3740.
[43] A. Fulton, How crowded is the cytoplasm?, Cell 30 (1982) 345–347
[44] O. Medalia, I. Weber, A.S. Frangakis, D. Nicastro, G. Gerisch, W. Baumeister, Macromolecular architecture in eukaryotic cells visualized by cryoeloctron tomography, Science 298 (2002) 1209–1213.
[45] C. Mattea, J. Qvist, B. Halle, Dynamics at the protein–water interface from ^{17}O spin relaxation in deeply supercooled solutions, Biophys. J. 95 (2008) 2951–2963.
[46] A.M. Stadler, J.P. Embs, I. Digel, G.M. Artmann, T. Unruh, G. Büldt, G. Zaccai, Cytoplasmic water and hydration layer dynamics in human red blood cells, J. Am. Chem. Soc. 130 (2008) 16852–16853.